Characteristics of magnesium-based hydrogen-storage alloy electrodes

N. Cui, B. Luan, H.K. Liu, H.J. Zhao, S.X. Dou

Centre for Superconducting and Electronic Materials, University of Wollongong, Northfields Avenue, Wollongong, NSW 2522, Australia

Abstract

Various Mg_2Ni-type hydrogen-storage alloy electrodes are prepared and characterized at room temperature. The discharge capacity is improved markedly via partial substitution of titanium for magnesium and iron for nickel in the Mg_2Ni alloy. Composites of Mg_2Ni with Ti_2Ni can also increase greatly the discharge capacity of the magnesium-based electrode. As a consequence, the magnesium-based hydrogen-storage alloys are promising materials for secondary batteries and may provide further improvements in capacity and cycling performance.

1. Introduction

Magnesium-based alloys are considered to be most promising materials for hydrogen-storage because of their high hydrogen-storage capacity, light weight, abundance of the constituents in the earth's crust, and low-cost compared with alternative systems. Of all the magnesium-based alloys, Mg_2Ni is the most remarkable due to its relative high capacity and favourable kinetics. It is well known that pure magnesium and Mg_2Ni can absorb up to 7.6 and 3.8 wt.% hydrogen, respectively [1]. These quantities are much higher than the capacities of either rare-earth system hydrogen-storage alloys (e.g., $LaNi_5$ absorbs 1.4 wt.% hydrogen) or titanium system hydrogen-storage alloys (e.g., TiFe absorbs 1.9 wt.% hydrogen) [2]. On the debit side, however, the reactions of magnesium–magnesium alloys with hydrogen require appreciably high temperatures (200–300 °C) and pressures (up to 10 atm) due to hydriding/dehydriding difficulties [3–5].

Numerous investigations have been conducted in order to improve the kinetics of magnesium and magnesium-based alloys. The approaches can be summarized as follows: (i) element substitutions; (ii) composite formation of magnesium and/or magnesium-based alloys with other hydrogen-storage alloys (e.g., rare-earth system or titanium system); (iii) addition of oxides, and (iv) surface modifications with metal coatings and or-

ganic/inorganic compounds. Nevertheless, the investigations have concentrated only on the hydriding/dehydriding characteristics of magnesium and magnesium-based alloys in the gas phase. As yet, no work has been directed towards the electrochemical performance of magnesium-based alloys. In the present study, magnesium-based hydrogen-storage alloy electrodes are prepared and investigated. Alloy composite and room temperature micro-encapsulation are applied to improve the performance of the electrodes.

2. Experimental

2.1. Alloy preparation

Mg_2Ni and $Mg_{1.8}Ni_{0.75}Ti_{0.2}Fe_{0.25}$ alloys were prepared from the constituent elements according to the conventional powder metallurgical technique as described in the following procedure. Pure metal powders (Aldrich Chemical Company, 99 + %) were thoroughly mixed and pressed into pellets in required stoichiometric ratios without binder. The pellets were then transferred into alumina boats and sintered in high purity argon atmosphere at 825 K for 50 h and at 900 K for 10 h after flushing with argon gas for several times. Composite alloy Mg_2Ni–10wt.%Ti_2Ni was synthesized by mixing

the prefabricated Ti₂Ni (as previously reported [6]) with Mg₂Ni, followed by the same procedure.

2.2. Electrode fabrication

The alloy pellets were crushed and pulverized mechanically into powder with an average particle size below 75 μm. The powder was micro-encapsulated using the low-temperature, surface technique that has been described previously [7]. Each coated/uncoated alloy powder was mixed with 20 wt.% TAB-3 (Teflon acetylene black composite binder), using a mortar and a pestle, to form a film. The resulting film was then pressed on both sides of a foam nickel sheet to form a sandwich electrode.

2.3. Charge/discharge procedures

Electrode properties were tested in 6 M KOH using an Hg/HgO electrode as reference electrode (all potentials are reported with respect to this electrode) and nickel sheet as a counter electrode. Charge/discharge was controlled by an automatic galvanostatic charge/discharge unit (DEC-1). The electrodes were charged to the gassing voltage, rested for 30 min, and then discharged galvanostatically to -0.50 V.

2.4. Phase analysis

The structure and phase analysis of the alloy powders were characterized by X-ray diffraction (XRD) using a Philips PW 1010 machine with Cu Kα radiation.

3. Results and discussion

3.1. Mg₂Ni alloy

The discharge capacities of various magnesium-based alloy electrodes are given in Table 1. The discharge capacity (8 mAh/g only) of the Mg₂Ni electrode fabricated from uncoated powder is almost negligible, while the electrode fabricated from Ni–P coated powder has a much higher discharge capacity (54 mAh/g). This indicates that surface micro-encapsulation at low tem-

perature is effective in improving the electrochemical performance of magnesium-based alloy electrodes, in a manner similar for Ti₂Ni electrodes reported in previous work [7]. The typical discharge characteristics of the electrode fabricated from the micro-encapsulated powder are shown in Figs. 1 and 2. As can be seen, the discharge capacity of the coated Mg₂Ni alloy electrode decreases rapidly over the first three cycles, and then remains almost constant from the fourth cycle onwards. This indicates that micro-encapsulation is beneficial in terms of reducing the capacity decay rate and improving the cycle life of Mg₂Ni electrodes.

It is well known that there are three types of Mg₂Ni hydrides, namely, Mg₂NiH₄, Mg₂NiH and Mg₂NiH₀.₃ [8]. The theoretical capacities of these compounds are given in Table 2. The experimental capacity values of the Mg₂Ni electrode are 8 mAh/g for an uncoated electrode and 56 mAh/g for a coated electrode. The measured capacities are much lower than the theoretical values. The reasons for this are as follows. First, the surface of Mg₂Ni alloy is usually contaminated by oxide and/or hydroxide layer when exposed in KOH solution. This surface layer may prohibit the reduction of H⁺
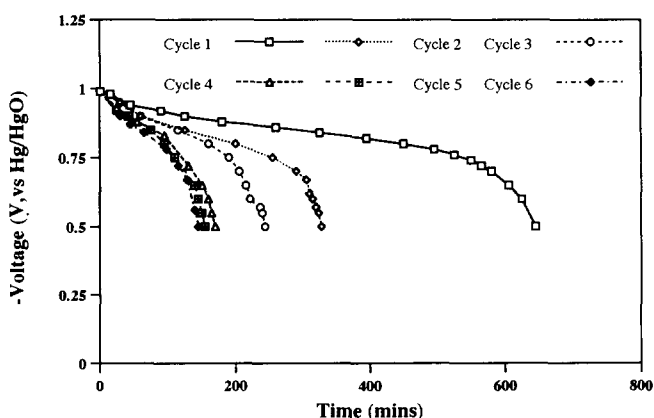
Table 1
Comparison of discharge capacities of various Mg₂Ni-type hydrogen-storage alloy electrodes (discharge at 5 mA/g)

Electrode	Discharge capacity (mAh/g)
Uncoated Mg₂Ni	8
Coated Mg₂Ni	54
Mg₁.₈Ti₀.₂Ni₀.₇₅Fe₀.₂₅	90
Mg₂Ni–10wt.%Ti₂Ni	126

Fig. 1. Galvanostatic discharge curves of a coated Mg₂Ni electrode (discharge at 5 mA/g).
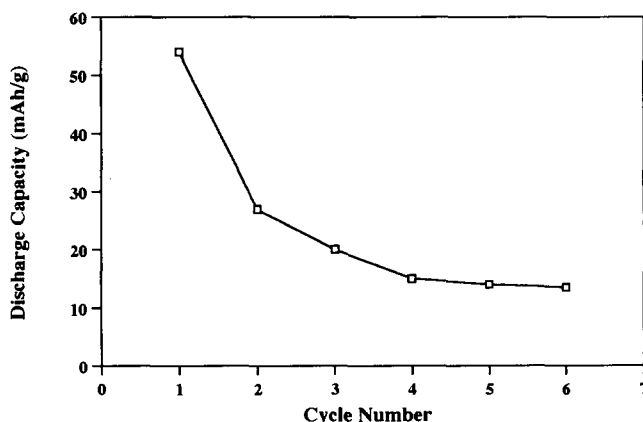
Fig. 2. Capacity decay of a coated Mg₂Ni electrode (discharge at 5 mA/g).
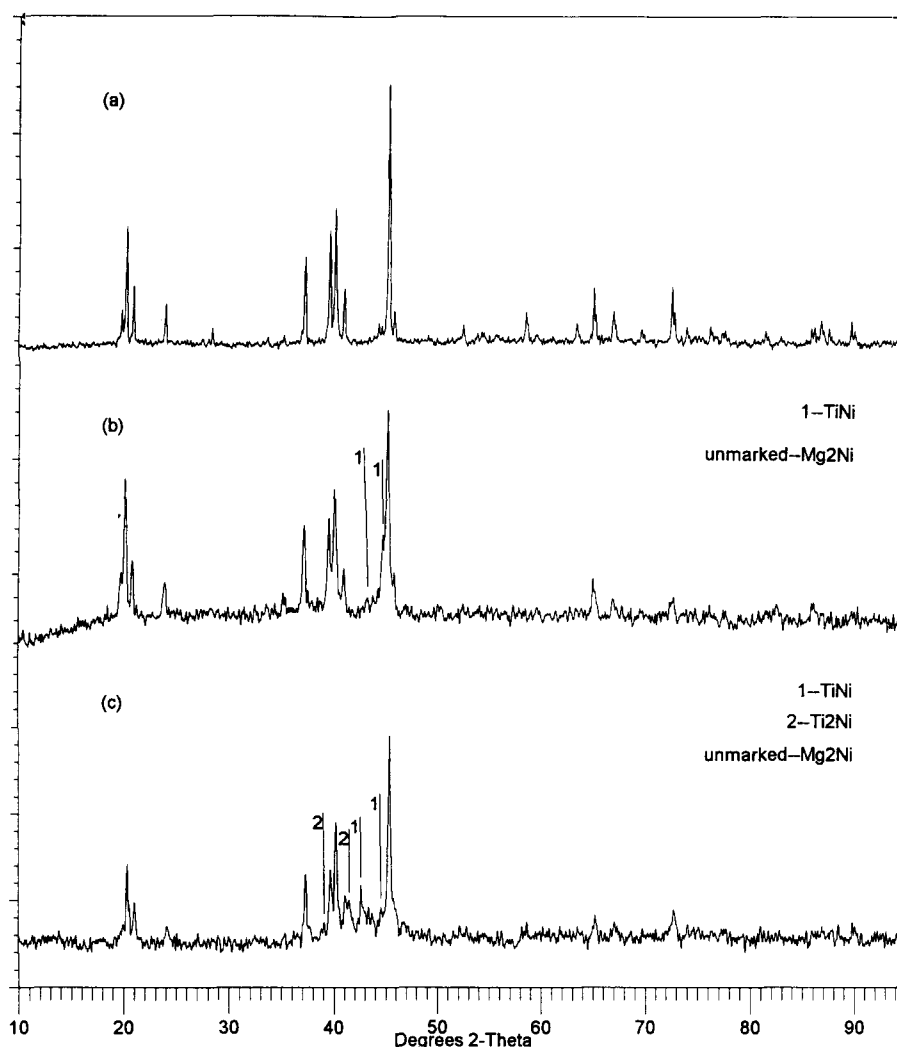
Fig. 3. X-ray diffraction patterns for magnesium-based alloy powders before cycling: (a) Mg_2Ni; (b) $Mg_{1.8}Ti_{0.2}Ni_{0.75}Fe_{0.25}$, and (3) Mg_2Ni–10wt.%Ti_2Ni.

Table 2
Theoretical capacities of Mg_2Ni hydride electrode

Electrode	Theoretical electrochemical capacity (mAh/g)
Mg_2NiH_4	999
Mg_2NiH	250
$Mg_2NiH_{0.3}$	75

ions on the electrode surface. Thus, the oxide and/or hydroxide layer formed on the surface of the electrode may inhibit the nucleation and the growth of the hydride phase during charging, and block the migration of hydrogen to the solution/electrode interface for discharging. Second, the hydride formed at the surface acts as diffusion barrier for hydrogen. The transport of hydrogen through the hydride layer is expected to be retarded since the diffusion of hydrogen in Mg_2NiH_x (low-temperature phase) is extremely slow. As a result, the thickness of the hydride layer is generally about

0.1 to 1 μm [9], which is much smaller than the alloy particle size (about 75 μm). Therefore, the Mg_2Ni electrode is only hydrided partially and a very low discharge capacity is obtained.

It is also well known that a Ni–P coating on an Mg_2Ni alloy powder surface can effectively protect the alloy from oxidation in KOH solution. Simultaneously, the coating acts as an electrocatalyst for hydrogen ion reduction [10], and thus is beneficial to the hydriding/dehydriding reactions and causes an improvement of the discharge capacity. Even if the electrode is fabricated from coated powder, once the hydride layer reaches a certain thickness, further growth of the hydride layer may become difficult. Therefore, the discharge capacity of the electrode fabricated from coated powder is greatly improved, but is still far from satisfactory.

3.2. $Mg_{1.8}Ti_{0.2}Ni_{0.75}Fe_{0.25}$ alloy

Numerous reports show that the hydriding and dehydriding reaction of a Mg_2Ni-type hydrogen-storage

alloy in the gas phase can be facilitated by elemental substitutions of Mg and/or Ni [3–5]. In the present work, $Mg_{1.8}Ti_{0.2}Ni_{0.75}Fe_{0.25}$ was chosen to investigate the electrode characteristics.

The XRD pattern of $Mg_{1.8}Ti_{0.2}Ni_{0.75}Fe_{0.25}$ powder is given in Fig. 3(b), and compared with that of the Mg_2Ni powder (Fig. 3(a)). The data of Fig. 3(b) show that two phases co-exist: a main phase with a hexagonal symmetry structure the same as the Mg_2Ni alloy, and a second phase, TiNi. According to Lupu et al. [11], iron can only partially replace nickel atoms. The remainder of the iron atoms are present as isolated atoms or clusters of small size.

Fig. 4 shows the discharge curves of a $Mg_{1.8}Ti_{0.2}Ni_{0.75}Fe_{0.25}$ electrode. It can be seen from Table 1 and Fig. 4 that the substitution of titanium for magnesium and iron for nickel in Mg_2Ni improves significantly the discharge capacity of the Mg_2Ni-type electrode. The discharge capacity is increased from 8 mAh/g for an uncoated Mg_2Ni electrode to 90 mAh/ g for a $Mg_{1.8}Ti_{0.2}Ni_{0.75}Fe_{0.25}$ electrode. The behaviour may be due to the electrochemical catalytic effect of the TiNi second phase and the isolated iron atoms or small-size iron clusters. The discharge curves and capacities at different discharge current densities are given in Figs. 5 and 6. The discharge capacity of a $Mg_{1.8}Ti_{0.2}Ni_{0.75}Fe_{0.25}$ electrode decreases quickly with increasing discharge current, and falls to only ~10 mAh/g at a discharge current density of 40 mA/g. This shows that the dehydriding rate of a Mg_2Ni-type alloy as an electrode in KOH solution is much slower than that of rare-earth system and titanium system hydrogen-storage alloys.

3.3. $Mg_2Ni–10wt.\%Ti_2Ni$ alloy

Fig. 3(c) shows the XRD pattern for the $Mg_2Ni–10wt.\%Ti_2Ni$ sintered composite. The results show that the composite is a multiphase system composed of Mg_2Ni, Ti_2Ni and TiNi.
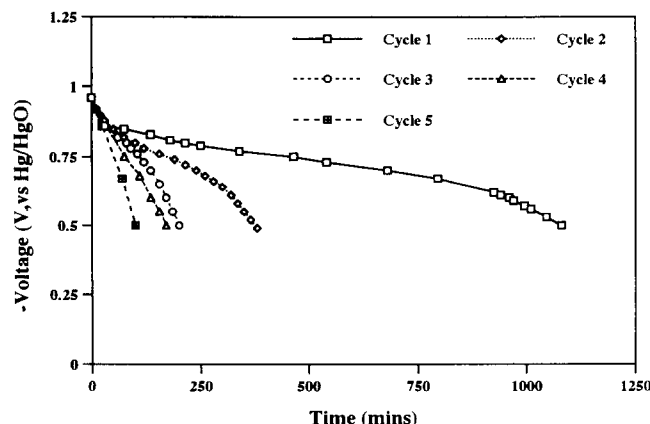
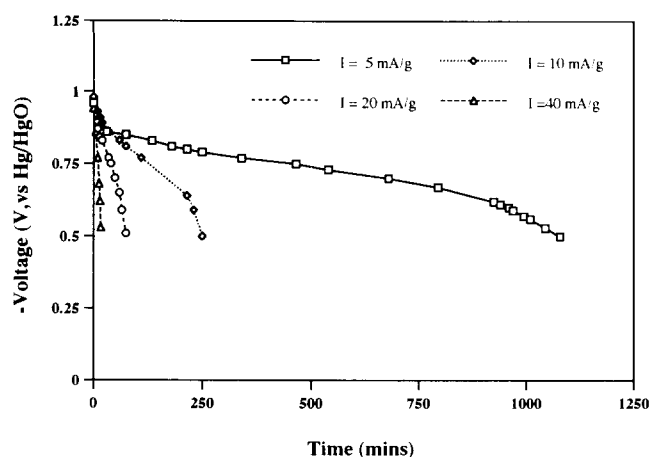Fig. 4. Galvanostatic discharge curves of $Mg_{1.8}Ti_{0.2}Ni_{0.75}Fe_{0.25}$ electrode (discharge at 5 mA/g).

Fig. 5. Galvanostatic discharge curves of a $Mg_{1.8}Ti_{0.2}Ni_{0.75}Fe_{0.25}$ electrode at different discharge currents.
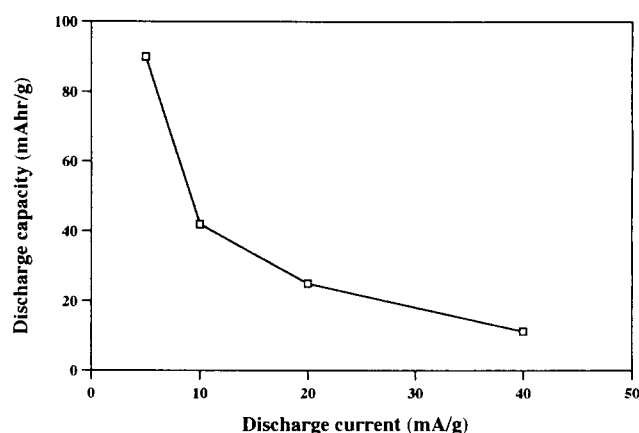
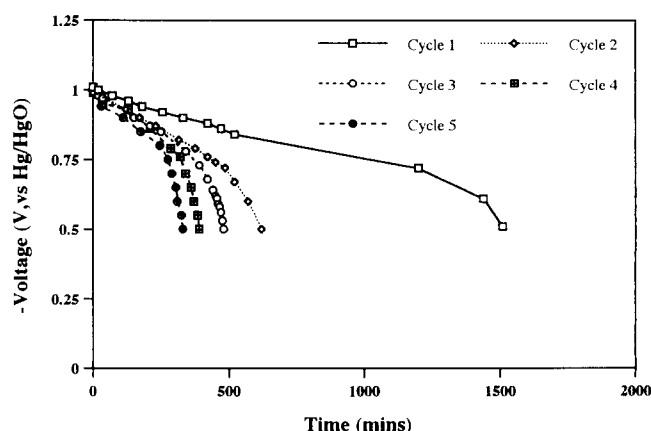Fig. 6. Discharge capacities of a $Mg_{1.8}Ti_{0.2}Ni_{0.75}Fe_{0.25}$ electrode at different discharge currents.

Fig. 7. Galvanostatic discharge curves of a $Mg_2Ni–10wt.\%Ti_2Ni$ electrode (discharge at 5 mA/g).

Fig. 7 presents the discharge curves of a $Mg_2Ni–10wt.\%Ti_2Ni$ composite electrode. The discharge capacity increases from 8 mAh/g for an uncoated Mg_2Ni electrode to 126 mAh/g. As reported [12], a

Ti$_2$Ni alloy has a much higher reaction rate with hydrogen than a Mg$_2$Ni alloy. Thus, as an additional phase, it may exert an important catalytic effect on the hydriding/dehydriding rate of the composite alloy and, therefore, enhance the discharge capacity.

4. Conclusions

Characterizations of Mg$_2$Ni-type hydrogen-storage alloy electrodes at room temperature have been performed for the first time. A discharge specific capacity of 126 mAh/g is obtained at a discharge current density of 5 mA/g from a composite electrode of Mg$_2$Ni and Ti$_2$Ni alloy powders. Substitution of titanium for magnesium and iron for nickel in Mg$_2$Ni also greatly improves the discharge capacity. This may be attributed to the electrochemical catalytic effects of the second phase that improve the electrode reaction rate and, thus, yield a remarkable enhancement of discharge capacity.

References

[1] J.C. Bolcich, A.A. Yawuy, H.L. Corso, H.A. Pertti and C.O. Anala, Int. J. Hydrogen Energy, 19 (1994) 605–609.

[2] K. Dutta, P. Mondal, K. Ramakrishna and O.N. Srivastava, Int. J. Hydrogen Energy, 19 (1994) 253–267.

[3] J.P. Darnaudery, B. Darriet and M. Pezat, Int. J. Hydrogen Energy, 8 (1983) 705–708.

[4] P. Sewam, B. Viswanathan, C.C. Swanny and V. Srinvasan, Int. J. Hydrogen Energy, 13 (1988) 82–89.

[5] P. Sewam, B. Viswanathan, C.C. Swanny and V. Srinvasan, Int. J. Hydrogen Energy, 10 (1986) 169–192.

[6] B. Luan, N. Cui, H.K. Liu, H.J. Zhao and S.X. Dou, J. Power Sources, in press.

[7] B. Luan, N. Cui, H.K. Liu, H.J. Zhao and S.X. Dou, J. Power Sources, 52 (1994) 295–299.

[8] JCPDS, Powder Diffraction File, 38-948, 40-1206, 40-1204, 1989.

[9] Y. Zhou, L.C. Erickson, B. Hjorvarsson, J. Alloys Compounds, 209 (1994) 117–124.

[10] J.J. Podesta, R.C.V. Pitti, A.J. Arvia, P. Ekdung, K. Juttner and G. Kreysa, Int. J. Hydrogen Energy, 17 (1992) 9–22.

[11] D. Lupu, A. Biris, E. Indrea, N. Aldea and R.V. Bucur, Int. J. Hydrogen Energy, 8 (1983) 797–799.

[12] B. Luan, N. Cui, H.K. Liu, H.J. Zhao and S.X. Dou, J. Power Sources, in press.